Letter

# Submicrosecond high-fidelity dispersive readout of a spin qubit with squeezed photons

Chon-Fai Kam and Xuedong Hu*
*Department of Physics, University at Buffalo, SUNY, Buffalo, New York 14260, USA*

(Received 18 December 2023; accepted 11 April 2024; published 29 April 2024)

Fast and high-fidelity qubit measurement is essential for realizing quantum error correction, a key ingredient to universal quantum computing. For electron spin qubits, fast readout is one of the significant challenges toward error correction. Here we examine the dispersive readout of a single spin in a semiconductor double quantum dot coupled to a microwave resonator. We show that using displaced squeezed vacuum states for the probing photons can improve the qubit readout fidelity and speed. With proper phase matching, moderate squeezing can enhance both the signal-to-noise ratio and the fidelity of the qubit readout, and the optimal readout time can be shortened to the submicrosecond range with above 97% fidelity. These enhancements are achieved at low probing microwave intensity, ensuring nondemolition qubit measurement.

DOI: 10.1103/PhysRevA.109.L040402

*Introduction*. Significant progress has been made toward building a universal quantum computer over the past decade based on a variety of qubit platforms [1–12]. Among these options, spin qubits in silicon quantum dots, while lagging somewhat behind other systems such as superconducting and trapped ion qubits [13,14], hold tantalizing long-term potential due to their excellent quantum coherence [5], a small qubit footprint, and compatibility with the well-established microelectronics industry [15]. Further development of spin qubits still faces a multitude of challenges. For example, a key element of scalable quantum computing is active quantum error correction (QEC) [16–18], which hinges on high-fidelity readout in times that are significantly shorter than the qubits' decoherence times [15]. For a spin qubit in isotopically purified silicon, spin dephasing time is typically of the order of tens of microseconds [5], making it crucial to attain readout fidelity above the 99% threshold of the surface code for QEC [19–21] in a submicrosecond timescale.

Commonly used spin measurement approaches based on spin-dependent tunneling [22] or spin blockade [23], together with a DC charge sensor, are too slow for active QEC. A radio frequency (rf) charge sensor, such as the rf single-electron transistor (rf-SET), could speed up the measurement, having achieved single-shot readout of a single-spin qubit with 97% fidelity in 1.5 μs [24] and 99.9% fidelity in 6 μs [25]. Recently, a single-shot singlet-triplet readout based on rf reflectometry has achieved a signal-to-noise ratio (SNR) of 6 in 0.8 μs [26], while another reached 99% fidelity in 1.6 μs [27]. However, a charge sensor adds to the complexity of a device, and the larger footprint of rf-SETs constrains their placement in highly connected qubit architectures [28]. Gate-reflectometry-based dispersive spin readout skips the charge sensor and sends the probing pulse directly to the qubit through one of its gates [29]. Using an off-chip resonator, readout fidelities ranging from 73.3% to 98% have been achieved, though achieving single-shot readout has so far required integration times of the order of milliseconds [30–32]. With an on-chip resonator and a microwave probe pulse, a single-shot readout fidelity of 98% has been achieved at a respectable 6 μs measurement time [33]. In short, fast readout with high fidelity and small footprint remains a formidable challenge for scalable quantum information processing based on spin qubits.

One approach to improve a reflectometry-based spin readout protocol is to employ squeezed states for photons in the measurement process. Squeezed states are nonclassical states with modified quantum noise profiles [34–36]. By introducing quantum correlations among photons, quantum fluctuations are periodically reduced to below the standard quantum limit in one field quadrature, while simultaneously increased in the conjugate quadrature [37]. Squeezed states have been extensively studied in various research fields. For instance, high-intensity squeezed light has been employed in the latest gravitational wave detectors [38,39], resulting in a nearly tenfold increase in sensitivity [40]. In the field of quantum information processing, a squeezed state has been applied in continuous-variable quantum key distribution [41], quantum sensing [42], and high-precision cavity spectroscopy [43]. Squeezed states have helped enhance the signal-to-noise ratio (SNR) of superconducting qubit readout [44], leading to a 24% increase in the final SNR for superconducting qubit measurement [45]. A 31% enhancement in the SNR for superconducting qubit readout with 99% fidelity was realized when a two-mode squeezed vacuum was used [46]. Squeezing has also been suggested for nondemolition qubit readout, achieving intracavity squeezing beyond the 3 dB limit [47], exponentially enhanced light-matter interaction [48], and shortcuts to adiabaticity for the quantum Rabi model [49].

Here we explore the impact of squeezing on the dispersive readout of a spin qubit coupled to an on-chip microwave resonator, and its subsequent backaction on the spin qubit (Fig. 1). We find that using a low-intensity (so as to reduce photon-induced decoherence) squeezed state could yield

*Corresponding author: xhu@buffalo.edu

 

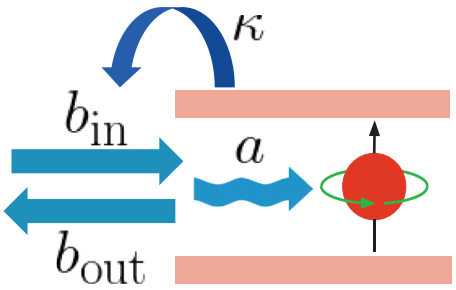


FIG. 1. Schematic of the setup for dispersive detection of spin qubits.

significant enhancements in the SNR, enabling rapid and high-fidelity dispersive readout of the spin qubit through standard techniques. Interestingly, we also find that only a modest degree of squeezing, under proper phase-matching conditions, improves spin measurement. Larger squeezing actually leads to a deterioration of measurement SNR and fidelity due to contributions from the "antisqueezed" quadrature.

*The model*. We consider dispersive readout of a spin qubit assisted by a single-mode microwave resonator. In the rotating frame, the dispersive coupling Hamiltonian between the qubit and the resonator field is [50]

$$H_s = \tfrac{1}{2}(\delta_s - \chi_s)\sigma_z + (\delta_c - \chi_s\sigma_z)a^\dagger a, \tag{1}$$

where $\delta_c$ and $\delta_s$ denote the detunings of the probe from the resonator and the spin qubit, respectively, and $\chi_s$ is the dispersive coupling strength between the spin qubit and the resonator. The photons can enter and leave the resonator through a single input-output port with a coupling rate $\kappa$, governed by an interaction of the form [50]

$$V_{\rm in} = i\sqrt{\kappa}(b_{\rm in}^\dagger a - b_{\rm in}a^\dagger), \tag{2}$$

where $b_{\rm in}$ and $b_{\rm in}^\dagger$ are the annihilation and creation operators of the input radiation field mode. From the effective Hamiltonian $H_{\rm eff} \equiv H_s + V_{\rm in}$ for the coupled qubit-photon system, the Langevin equation for the resonator field takes the form

$$\dot{a} = -\left[i(\delta_c - \chi_s\sigma_z) + \frac{\kappa}{2}\right]a - \sqrt{\kappa}b_{\rm in}, \tag{3}$$

where the first term on the right-hand side describes the dispersive shift of the resonator field as well as damping, while the last term represents the driving of the resonator through its input port. The damping term in Eq. (3) is a result of the Markovian approximation, depending solely on the system operators at the current time. It forms the basis of the input-output theory [51,52]. Under the Markovian approximation, the output radiation field mode is given by [51]

$$b_{\rm out} = b_{\rm in} + \sqrt{\kappa}a, \tag{4}$$

where $b_{\rm out}$ and $b_{\rm out}^\dagger$ are the annihilation and creation operators of the output radiation field mode, respectively. To ensure the commutation relation $[b_{\rm out}, b_{\rm out}^\dagger] = [b_{\rm in}, b_{\rm in}^\dagger]$, $[b_{\rm in}^\dagger, a] = [a^\dagger, b_{\rm in}] = \frac{\sqrt{\kappa}}{2}[a, a^\dagger]$ are required [51].

The Langevin equation (3) and the input-output relation (4) form the basis of our study. The former describes how the resonator field is affected by the qubit and the pumping from the outside, while the latter relates the reflected field to the input and the resonator field, allowing us to evaluate how the qubit state affects the output. When the qubit-resonator interaction is dispersive, the spin measurement becomes nondestructive when the resonator field is weak, wherein $\sigma_z(t)$ is approximately a constant of motion: $\sigma_z(t) \approx \sigma_z(0)$. Consequently, $\sigma_z$ can be represented as a real number $\sigma = \pm 1$, allowing for an analysis of the readout contrast. Without loss of generality, we assume $\delta_c = 0$ from now on.

In rf reflectometry, the output field $b_{\rm out}$ is sent through a phase-preserving amplifier [53], which detects both quadratures equally well and is subsequently measured using a homodyne detector [54] by mixing with a local oscillator with phase $\varphi$. The resulting photocurrent $I \propto \frac{1}{\sqrt{2}}(b_{\rm out}e^{-i\varphi} + b_{\rm out}^\dagger e^{i\varphi})$. By properly choosing the local oscillator phase, the photocurrent could be proportional to any field quadrature, such as $Q_{\rm out} \equiv \frac{1}{\sqrt{2}}(b_{\rm out} + b_{\rm out}^\dagger)$ or $P_{\rm out} \equiv \frac{1}{\sqrt{2}i}(b_{\rm out} - b_{\rm out}^\dagger)$. We thus rewrite the resonator Langevin equation in terms of their quadratures as

$$\dot{X}(t) = MX(t) - \sqrt{\kappa}X_{\rm in}, \quad M \equiv -\frac{\kappa}{2}I \mp i\chi_s\tau_y, \tag{5}$$

where $X \equiv (Q, P)^\top$ is the column vector of the two orthogonal quadratures for the resonator field, $X_{\rm in} \equiv (Q_{\rm in}, P_{\rm in})^\top$, and $\tau_y$ is the $y$-Pauli matrix in the field quadrature subspace. Here, $Q$ and $P$ are referred to as the amplitude and phase quadratures of the resonator field, and $Q_{\rm in}$ and $P_{\rm in}$ are those of the input field. For a continuous wave input, the resonator field quadratures are obtained as

$$X(t) = e^{Mt}X(0) - \sqrt{\kappa}\int_0^t ds e^{Ms}X_{\rm in}, \tag{6}$$

where $e^{Mt} = f(t)I \mp ig(t)\tau_y$, $f(t) \equiv e^{-\frac{\kappa}{2}t}\cos\chi_s t$, and $g(t) \equiv e^{-\frac{\kappa}{2}t}\sin\chi_s t$. Substituting this result into Eq. (4) would then yield the solutions for the output field quadratures.

*Signal-to-noise ratio*. Recall that in rf reflectometry, the homodyne measurement yields a photocurrent that is proportional to the expectation value of an output field quadrature. Without loss of generality, we choose the output quadrature as $P_{\rm out} \equiv P_{\rm in} + \sqrt{\kappa}P$, which is specified by a local oscillator phase of $\pi/2$. To quantify the distinguishability between the two qubit states, we introduce the signal-to-noise ratio (SNR) defined as

$$\mathrm{SNR}(t) \equiv \frac{|\langle\mathscr{M}^{+1}(t)\rangle - \langle\mathscr{M}^{-1}(t)\rangle|}{\Delta\mathscr{M}^{+1}(t) + \Delta\mathscr{M}^{-1}(t)}. \tag{7}$$

Here, $\langle\mathscr{M}^{\pm}(t)\rangle$ and $\Delta\mathscr{M}^{\pm}(t)$ are the expectation values and standard derivations, respectively, of the time-integrated output quadratures $\mathscr{M}^{\pm}(t) \equiv \int_0^t P_{\rm out}^{\pm}(s)ds$, where the superscript refers to the two qubit states. $\mathscr{M}^{\pm}(t)$ takes the explicit form

$$\mathscr{M}^{\pm}(t) = A(t)P_{\rm in} \mp B(t)Q_{\rm in} + \sqrt{\kappa}F(t)P(0) \pm \sqrt{\kappa}G(t)Q(0), \tag{8}$$

where the time-dependent coefficients are $A(t) \equiv t - \kappa\int_0^t F(s)ds$, $B(t) \equiv \kappa\int_0^t G(s)ds$, $F(t) \equiv \int_0^t f(s)ds$, and $G(t) \equiv \int_0^t g(s)ds$. Interestingly, when the resonator field is initially in a vacuum state, the contrast between the output signals is given by $2|B(t)\langle Q_{\rm in}\rangle|$, which depends solely on the input quadrature $Q_{\rm in}$ and is independent of $P_{\rm in}$.

Now we are ready to explore the effect of squeezing in the input field. We choose a displaced squeezed vacuum state $|\boldsymbol{\alpha}, \boldsymbol{\xi}\rangle \equiv D(\boldsymbol{\alpha})S(\boldsymbol{\xi})|0\rangle$ as an input, where $D(\boldsymbol{\alpha}) \equiv \exp \int dk(\alpha_k b_k^\dagger - \alpha_k^* b_k)$ is a continuous displacement operator, and $S(\boldsymbol{\xi}) \equiv \exp \frac{1}{2} \int dk(\xi_k^* b_k^2 - \xi_k b_k^{\dagger 2})$ is a continuous squeezing operator [55,56]. Here, $\boldsymbol{\alpha} = \alpha e^{i\theta_\alpha}$ and $\boldsymbol{\xi} = \xi e^{i\theta_\xi}$. In this state, the expectation values of the annihilation and creation operators coincide with those of the coherent states: $\langle b_{\rm in}\rangle = \alpha(t)$ and $\langle b_{\rm in}^\dagger\rangle = \alpha^*(t)$ (see Supplemental Material [57]).

For a homodyne detection with a local oscillator phase $\varphi = \pi/2$, the signal contrast is proportional to $|\cos\theta_\alpha|$. To maximize this contrast, $\theta_\alpha$ must vanish. For time shorter than $2/\kappa$, one can make the approximations $A(t) \approx t - \frac{1}{2}\kappa t^2$ and $B(t) \approx \frac{1}{6}\kappa\chi_s t^3$. Consequently, during a fast dispersive readout, the noise from the input quadrature $P_{\rm in}$ when leaving the resonator largely exceeds that from $Q_{\rm in}$. To enhance the SNR, it is thus beneficial to choose $P_{\rm in}$ as the squeezed quadrature, associated with $\theta_\xi = \pm\pi$, which leads to

$$[\Delta\mathscr{M}^{\pm}(t)]^2 = \frac{e^{-2r}}{2}A^2(t) + \frac{e^{2r}}{2}B^2(t) + \frac{\kappa}{2}[F^2(t) + G^2(t)]. \tag{9}$$

For a fixed value of squeezing amplitude $r$, the optimal readout time is $t \approx e^{-r}(6/\kappa\chi_s)^{1/2}$.

In general, in a homodyne detection setup with an arbitrary local oscillator phase $\varphi$, the SNR of the chosen quadrature is still determined by Eq. (9), but with $B(t)$ and $A(t)$ replaced by $B(t)\cos\Delta\theta + A(t)\sin\Delta\theta$ and $-B(t)\sin\Delta\theta + A(t)\cos\Delta\theta$, respectively. Here, $\Delta\theta \equiv \varphi - \theta_\xi/2$ is the phase mismatch between the local oscillator and the squeezing. In this general scenario, the signal contrast is proportional to $|\sin(\theta_\alpha - \varphi)|$. To maximize the contrast between the output signals, the phase of the displacement amplitude should lead or lag that of the local oscillator by $\pi/2$. Meanwhile, to minimize the noise from the input quadratures, the phase mismatch between the local oscillator and the squeezed state should be an integer multiple of $\pi$. Hence, the optimal SNR enhancement is characterized by the phase-matching relations

$$\theta_\alpha - \varphi = \left(m + \frac{1}{2}\right)\pi \quad \text{and} \quad \varphi - \frac{\theta_\xi}{2} = m'\pi, \tag{10}$$

where $m$ and $m'$ are arbitrary integers. Equation (10) immediately leads to a constraint on the phases of squeezing parameter $\xi$ and displacement $\alpha$: $2\theta_\alpha - \theta_\xi = [2(m + m') + 1]\pi$, which is required for squeezing to help enhance the SNR for qubit readout.

*Fidelity*. When the standard derivations of the time-integrated output quadratures are equal $[\Delta\mathscr{M}^+(t) = \Delta\mathscr{M}^-(t)]$, the single-shot readout fidelity $\mathscr{F}(t)$ is determined exclusively by the SNR as $\mathscr{F}(t) = \mathrm{erf}[\mathrm{SNR}(t)/\sqrt{2}]$, where $\mathrm{erf}z$ is the error function [61]. For qubits with a spin relaxation time $T_1$, the single-shot readout fidelity at time $t \ll T_1$ is given by

$$\mathscr{F}(t) = \exp\left(-\frac{t}{2T_1}\right)\mathrm{erf}\left(\frac{\mathrm{SNR}(t)}{\sqrt{2}}\right). \tag{11}$$

It incorporates both the relaxation of the qubit and the impact of the photon noise on the readout. Notably, the single-shot readout fidelity depends only on the spin relaxation time $T_1$, as the dispersive Hamiltonian (1) involves only the population difference between the two qubit states.

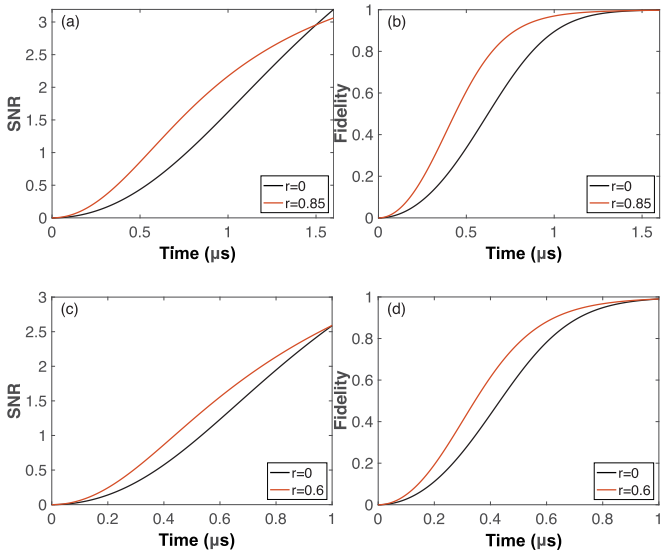


FIG. 2. SNR and readout fidelity with respect to different squeezing parameters and coupling rates. Here, $\alpha = \sqrt{30}$, $\chi_s/2\pi \equiv 0.15$ MHz, $\theta_\xi = \pi$, and $T_1 = 3$ ms [50]. The coupling rates are (a), (b) $\kappa = \chi_s$ and (c), (d) $\kappa = 2\chi_s$. The black (lower) lines represent the coherent state inputs.

*The results*. Figure 2 shows that employing squeezing for probing photons can enhance SNR and reduce measurement time. Here the black curves are for a coherent state input, setting the benchmark for comparison. Figure 2(a) reveals that using current technology ($\kappa/2\pi = \chi_s/2i = 0.15$ MHz) and a displaced squeezed vacuum state (with $\theta_\alpha = 0$ and $\theta_\xi = \pi$) as input, there is a clear SNR enhancement in the submicrosecond temporal regime. For example, there is a nearly 50% enhancement in the SNR at around 0.9 μs, or a 20% reduction in detection time for SNR around 1.5, achieved with around 30 photons and a moderate squeezing parameter of $r = 0.85$ (about 7.38 dB). Figure 2(b) shows that the chosen displaced squeezed vacuum state yields a notable readout fidelity of 97% at around 1 μs. Figure 2(c) indicates that by increasing the coupling rate slightly to $\kappa = 2\chi_s$, the same SNR can be achieved within an even shorter measurement time. Consequently, as shown in Fig. 2(d), a readout fidelity of 97% is attained at around 0.8 μs.

In Fig. 3, we show that a phase mismatch between the local oscillator and the squeezed state consistently lowers both the SNR and fidelity. At a fixed measurement time $t \approx 0.714$ μs and a fixed squeezing $r \approx 0.74$, the SNR increases from 3 to 3.5 compared to a coherent state input by fixing $\Delta\theta$ as a multiple of $\pi$, while a phase mismatch could reduce SNR to below 2 [Fig. 3(a)]. On the other hand, with the same measurement time $t \approx 0.714$ μs and for a perfect phase match of $\Delta\theta = \varphi - \theta_\xi/2 = 0$, the SNR increases as $r$ increases from 0, but then peaks at $r \approx 0.74$ (equivalent to 6.43 dB in decibels). Further increasing squeezing would then lead to a reduction in SNR. Both of these trends for SNR in Figs. 3(a) and 3(b) are closely followed by measurement fidelity as well, as shown in Figs. 3(c) and 3(d).

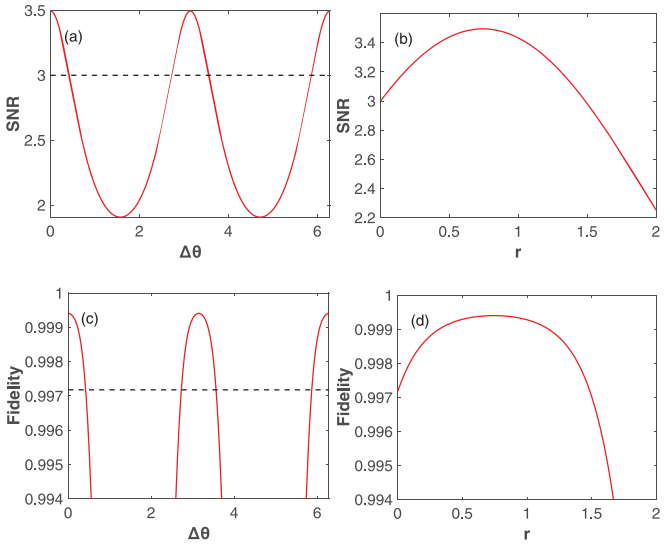


FIG. 3. SNR and readout fidelity with respect to different phase mismatches and squeezing parameters at a fixed measurement time $t \approx 0.714$ μs. Here, $|\alpha| = 10$, $\kappa = 2\chi_s$, $\chi_s/2\pi \equiv 0.15$ MHz, and $T_1 = 3$ ms. (a), (c) A squeezing parameter of $r = 0.74$ is chosen, and the black dashed lines represent the coherent state inputs. (b), (d) The phase-matching condition is given by $\Delta\theta \equiv \phi - \theta_\xi/2 = 0$.

The results in Fig. 3 challenge the seemingly reasonable assumption that measurement accuracy can continue to improve as the degree of squeezing increases. What we find here is that in a quantum measurement with a single-mode photonic state and a small number of photons, the contributions from the antisqueezing quadrature to the signal and noise are unavoidable. These contributions lead to the eventual decline of SNR and measurement fidelity as squeezing parameter $r$ increases. While the utilization of two or more photon modes theoretically allows for a higher signal-to-noise ratio by selecting two commuting quadratures, it could pose further challenges through intricate circuit architecture demands, such as incorporating two modes with opposing dispersive coupling constants [62–64].

The required squeezing in the current proposal is well within reach of the current state-of-the-art microwave experiments, where squeezing factor ranges from a few decibels to several dozens of decibels have been achieved. For instance, a squeezed microwave with a squeezing factor of up to 8 dB has been reported using a mechanical oscillator [65], while a broadband squeezed microwave radiation with a squeezing factor of up to 11.35 dB for a single-mode field has been reported using a Josephson traveling-wave parametric amplifier [66].

While all our calculations here are done with a displaced squeezed vacuum state for the input photons, a squeezed coherent state works as well, with the same phase-matching condition $\theta_\xi - 2\theta_\alpha = \pm\pi$. To achieve the same SNR and fidelity, the squeezed coherent state $|\xi, \gamma\rangle$ needs to have a modified displacement amplitude, $\gamma = \alpha e^{-r}$.

*Backaction on the qubit*. In the above discussion, we assume that qubit properties such as its relaxation time are not affected by the probing photons. Such an assumption is reasonable considering that we work with weak-intensity probing photons. Nevertheless, we now analyze how these photons, especially their squeezing, may affect qubit relaxation. For an accurate examination of spin relaxation, we revisit the original spin-photon coupling Hamiltonian, which describes the direct energy exchange between the spin qubit and the resonator via the absorption or emission of a resonator photon. Up to the leading order in spin-photon coupling $g_s$, the effective coupling Hamiltonian takes the following form [50]: $i\sqrt{\kappa} g_s \Delta^{-1}(b_{\rm in}^+ \sigma_- - b_{\rm in}\sigma_+)$, where $\Delta$ is the spin-resonator detuning. A straightforward calculation yields (see Supplemental Material [57])

$$\frac{1}{T_1} = 2\gamma_{pu} \cosh 2r, \tag{12}$$

where $\gamma_{pu} \equiv \kappa g_s^2 \Delta^{-2}$ is the Purcell relaxation rate, characterizing the emission of a resonator photon into the environment. Equation (12) shows that the qubit relaxation rate is proportional to the Purcell relaxation rate, as expected, but is modified by the presence of squeezing. Specifically, the relaxation rate increases monotonically with the degree of squeezing, regardless of the displacement amplitude $|\alpha|$ when $|\alpha|^2 \ll n_c = \Delta^2/4g_s^2$ [50]. For $r = 1$, one obtains $T_1^{-1} \approx 7.52\gamma_{pu}$. For a stronger probe, there would be further corrections to the total relaxation rate due to spin transitions induced by probe photons.

*Conclusion*. In this study, we have demonstrated the effectiveness of employing displaced squeezed vacuum states to enhance the readout fidelity and reduce the readout time for a single spin in a semiconductor double quantum dot through dispersive coupling to a resonator. The key for squeezing to help enhance detection efficiency lies in a set of phase-matching conditions among the squeezing phase, the coherent displacement phase, and the local oscillator phase during homodyne detection. When these phase-matching conditions are met, a moderate degree of squeezing (a few decibels) proves effective in reducing the spin readout time to the submicrosecond range while maintaining high readout fidelity. For instance, with current technology ($\kappa/2\pi = \chi_s/2\pi \approx 0.15$ MHz), using a displaced squeezed vacuum state with 30 photons and a moderate squeezing parameter of $r = 0.85$ (∼7.38 dB) allows us to achieve a readout fidelity of 97% within a readout time of about 1 μs. With a slightly larger coupling rate for the resonator ($\kappa = 2\chi_s$), the same readout fidelity can be attained in approximately 0.8 μs. Interestingly, we also find that squeezing beyond a certain threshold starts to hinder rather than help spin measurement, due to the inevitable contribution from the antisqueezing quadrature to both the signal and noise because of our constraints of fast measurement using a low-intensity microwave. In comparison, superconducting transmon qubits have demonstrated readout fidelity of 98–99% for integration times below 100 ns because of their strong electric coupling to resonators [67]. Similarly, if the dispersive coupling strength of the spin qubit can be increased by an order of magnitude, i.e., $\chi_s/2\pi \approx 2.1$ MHz, while maintaining $\kappa = \chi_s$, a fidelity of 90% could also be achievable for a shorter integration time of 200 ns. Hence, within contemporary spin-resonator coupling schemes grounded on charge-photon interaction, the optimization of charge-photon coupling emerges as the foremost strategy for quantum dots [68].

*Acknowledgments.* We acknowledge financial support by U.S. ARO via Grants No. W911NF1710257 and No. W911NF2310018. We gratefully acknowledge valuable discussions with Bill Coish.

[1] M. Kjaergaard, M. E. Schwartz, J. Braumüller, P. Krantz, J. I.-J. Wang, S. Gustavsson, and W. D. Oliver, Annu. Rev. Condens. Matter Phys. **11**, 369 (2020).
[2] Q. Chen, M. Plasencia, Z. Li, S. Mukherjee, D. Patra, C.-L. Chen, T. Klose, X.-Q. Yao, A. A. Kossiakoff, L. Chang, P. C. Andrews , and J. J. G. Tesmer, Nature (London) **595**, 600 (2021).
[3] C. D. Bruzewicz, J. Chiaverini, R. McConnell, and J. M. Sage, Appl. Phys. Rev. **6**, 021314 (2019).
[4] K. Wright, K. M. Beck, S. Debnath, J. M. Amini, Y. Nam, N. Grzesiak, J. S. Chen, N. C. Pisenti, M. Chmielewski, C. Collins *et al.*, Nat. Commun. **10**, 1 (2019).
[5] G. Burkard, T. D. Ladd, J. M. Nichol, A. Pan, and J. R. Petta, Rev. Mod. Phys. **95**, 025003 (2023).
[6] A. Noiri, K. Takeda, T. Nakajima, T. Kobayashi, A. Sammak, G. Scappucci, and S. Tarucha, Nature (London) **601**, 338 (2022).
[7] X. Xue, M. Russ, N. Samkharadze, B. Undseth, A. Sammak, G. Scappucci, and L. M. K. Vandersypen, Nature (London) **601**, 343 (2022).
[8] M. T. Mądzik, S. Asaad, A. Youssry, B. Joecker, K. M. Rudinger, E. Nielsen, K. C. Young, T. J. Proctor, A. D. Baczewski, A. Laucht *et al.*, Nature (London) **601**, 348 (2022).
[9] K. Takeda, A. Noiri, T. Nakajima, T. Kobayashi, and S. Tarucha, Nature (London) **608**, 682 (2022).
[10] S. Takeda, and A. Furusawa, APL Photon. **4**, 060902 (2019).
[11] J. E. Bourassa, R. N. Alexander, M. Vasmer, A. Patil, L. Tzitrin, T. Matsuura, D. Su, B. Q. Baragiola, S. Guha, G. Dauphinais *et al.*, Quantum **5**, 392 (2021).
[12] L. S. Madsen, F. Laudenbach, M. F. Askarani, F. Rortais, T. Vincent, J. F. F. Bulmer, F. M. Miatto, L. Neuhaus, L. G. Helt, M. J. Collins *et al.*, Nature (London) **606**, 75 (2022).
[13] L. Egan, D. M. Debroy, C. Noel, A. Risinger, D. Zhu, D. Biswas, M. Newman, M. Li, K. R. Brown, M. Cetina *et al.*, Nature (London) **598**, 281 (2021).
[14] H. Riel, *ESSDERC 2022 – IEEE 52nd European Solid-State Device Research Conference (ESSDERC)* (IEEE, Milan, Italy, 2022), pp. 25–30.
[15] M. F. Gonzalez-Zalba, S. de Franceschi, E. Charbon, T. Meunier, M. Vinet, and A. S. Dzurak, Nat. Electron. **4**, 872 (2021).
[16] J. Cramer, N. Kalb, M. A. Rol, B. Hensen, M. S. Blok, M. Markham, D. J. Twitchen, R. Hanson, and T. H. Taminiau, Nat. Commun. **7**, 11526 (2016).
[17] B. M. Terhal, Rev. Mod. Phys. **87**, 307 (2015).
[18] A. Saraiva and S. D. Bartlett, Nat. Mater. **22**, 157 (2023).
[19] T. Wu and J. Guo, in *IEEE Electron Device Letters*, Vol. 41, pp. 1078–1081.
[20] R. Raussendorf and J. Harrington, Phys. Rev. Lett. **98**, 190504 (2007).
[21] A. G. Fowler, M. Mariantoni, J. M. Martinis, and A. N. Cleland, Phys. Rev. A **86**, 032324 (2012).
[22] J. M. Elzerman, R. Hanson, L. H. Willems van Beveren, B. Witkamp, L. M. K. Vandersypen, and L. P. Kouwenhoven, Nature (London) **430**, 431 (2004).
[23] J. R. Petta, A. C. Johnson, J. M. Taylor, E. A. Laird, A. Yacoby, M. D. Lukin, C. M. Marcus, M. P. Hanson, and A. C. Gossard, Science **309**, 2180 (2005).
[24] D. Keith, M. G. House, M. B. Donnelly, T. F. Watson, B. Weber, and M. Y. Simmons, Phys. Rev. X **9**, 041003 (2019).
[25] M. J. Curry, M. Rudolph, T. D. England, A. M. Mounce, R. M. Jock, C. Bureau-Oxton, P. Harvey-Collard, P. A. Sharma, J. M. Anderson, D. M. Campbell *et al.*, Sci. Rep. **9**, 16976 (2019).
[26] A. Noiri, K. Takeda, J. Yoneda, T. Nakajima, T. Kodera, and S. Tarucha, Nano Lett. **20**, 947 (2020).
[27] E. J. Connors, J. J. Nelson, and J. M. Nichol, Phys. Rev. Appl. **13**, 024019 (2020).
[28] M. De Michielis, E. Ferraro, E. Prati, L. Hutin, B. Bertrand, E. Charbon, D. J. Ibberson, and M. F. Gonzalez-Zalba, J. Phys. D **56**, 363001 (2023).
[29] X. D. Hu, Nat. Nanotechnol. **14**, 735 (2019).
[30] P. Pakkiam, A. V. Timofeev, M. G. House, M. R. Hogg, T. Kobayashi, M. Koch, S. Rogge, and M. Y. Simmons, Phys. Rev. X **8**, 041032 (2018).
[31] A. West, B. Hensen, A. Jouan, T. Tanttu, C. H. Yang, A. Rossi, M. F. Gonzalez-Zalba, F. Hudson, A. Morello, D. J. Reilly *et al.*, Nat. Nanotechnol. **14**, 437 (2019).
[32] M. Urdampilleta, D. J. Niegemann, E. Chanrion, B. Jadot, C. Spence, P. A. Mortemousque, C. Bäuerle, L. Hutin, B. Bertrand, S. Barraud *et al.*, Nat. Nanotechnol. **14**, 737 (2019).
[33] G. Zheng, N. Samkharadze, M. L. Noordam, N. Kalhor, D. Brousse, A. Sammak, G. Scappucci, and L. M. K. Vandersypen, Nat. Nanotechnol. **14**, 742 (2019).
[34] D. F. Walls, Nature (London) **306**, 141 (1983).
[35] W. M. Zhang, R. Gilmore, and D. H. Feng, Rev. Mod. Phys. **62**, 867 (1990).
[36] C. F. Kam, W. M. Zhang, and D. H. Feng, *Coherent States: New Insights into Quantum Mechanics with Applications* (Springer Nature, Berlin, 2023).
[37] U. L. Andersen, T. Gehring, C. Marquardt, and G. Leuchs, Phys. Scr. **91**, 053001 (2016).
[38] M. Tse, H. Yu, N. Kijbunchoo, A. Fernandez-Galiana, P. Dupej, L. Barsotti, C. D. Blair, D. D. Brown, S. E. Dwyer, A. Effler *et al.*, Phys. Rev. Lett. **123**, 231107 (2019).
[39] F. Acernese, M. Agathos, L. Aiello, A. Allocca, A. Amato, S. Ansoldi, S. Antier, M. Arène, N. Arnaud, S. Ascenzi *et al.*, Phys. Rev. Lett. **123**, 231108 (2019).
[40] S. E. Dwyer, G. L. Mansell, and L. McCuller, Galaxies **10**, 46 (2022).
[41] T. Gehring, V. Händchen, J. Duhme, F. Furrer, T. Franz, C. Pacher, R. F. Werner, and R. Schnabel, Nat. Commun. **6**, 8795 (2015).
[42] B. J. Lawrie, P. D. Lett, A. M. Marino, and R. C. Pooser, ACS Photon. **6**, 1307 (2019).
[43] J. Junker, D. Wilken, E. Huntington, and M. Heurs, Opt. Express **29**, 6053 (2021).
[44] S. Barzanjeh, D. P. DiVincenzo, and B. M. Terhal, Phys. Rev. B **90**, 134515 (2014).

[45] A. Eddins, S. Schreppler, D. M. Toyli, L. S. Martin, S. Hacohen-Gourgy, L. C. G. Govia, H. Ribeiro, A. A. Clerk, and I. Siddiqi, Phys. Rev. Lett. **120**, 040505 (2018).
[46] G. Liu, X. Cao, T. C. Chien, C. Zhou, P. Lu, and M. Hatridge, Phys. Rev. Appl. **18**, 064092 (2022).
[47] W. Qin, A. Miranowicz, P. B. Li, X. Y. Lü, J. Q. You, and F. Nori, Phys. Rev. Lett. **120**, 093601 (2022).
[48] W. Qin, A. Miranowicz, and F. Nori, Phys. Rev. Lett. **129**, 123602 (2022).
[49] Y. H. Chen, W. Qin, X. Wang, A. Miranowicz, and F. Nori, Phys. Rev. Lett. **126**, 023602 (2021).
[50] B. D'Anjou and G. Burkard, Phys. Rev. B **100**, 245427 (2019).
[51] C. W. Gardiner and M. J. Collett, Phys. Rev. A **31**, 3761 (1985).
[52] C. Gardiner and P. Zoller, *Quantum Noise* (Springer, New York, 2004).
[53] A. A. Clerk, M. H. Devoret, S. M. Girvin, F. Marquardt, and R. J. Schoelkopf, Rev. Mod. Phys. **82**, 1155 (2010).
[54] H. P. Yuen, and V. W. S. Chan, Opt. Lett. **8**, 177 (1983).
[55] K. G. Fedorov, L. Zhong, S. Pogorzalek, P. Eder, M. Fischer, J. Goetz, E. Xie, F. Wulschner, K. Inomata, T. Yamamoto, Y. Nakamura, R. Di Candia, U. Las Heras, M. Sanz, E. Solano, E. P. Menzel, F. Deppe, A. Marx, and R. Gross, Phys. Rev. Lett. **117**, 020502 (2016).
[56] L. Mandel and E. Wolf, *Optical Coherence and Quantum Optics* (Cambridge University Press, Cambridge, 1995).
[57] See Supplemental Material at http://link.aps.org/supplemental/10.1103/PhysRevA.109.L040402 for detailed derivations. The Supplemental Material also contains Refs. [58–60].
[58] M. O. Hecht, A. J. Cobarrubia, and K. M. Sundqvist, IEEE Trans. Quantum Eng. **2**, 4100508 (2021).
[59] J. Zhang, Y. X. Liu, R. B. Wu, K. Jacobs, and F. Nori, Phys. Rev. A **87**, 032117 (2013).
[60] J. Combes, J. Kerckhoff, and M. Sarovar, Adv. Phys. X **2**, 784 (2017).
[61] M. Abramowitz and I. A. Stegun, *Handbook of Mathematical Functions with Formulas, Graphs, and Mathematical Tables* (Dover, New York, 1972).
[62] N. Didier, A. Kamal, W. D. Oliver, A. Blais, and A. A. Clerk, Phys. Rev. Lett. **115**, 093604 (2015).
[63] L. C. G. Govia and A. A. Clerk, New J. Phys. **19**, 023044 (2017).
[64] N. Didier, J. Bourassa, and A. Blais, Phys. Rev. Lett. **115**, 203601 (2015).
[65] C. F. Ockeloen-Korppi, E. Damskägg, J. M. Pirkkalainen, T. T. Heikkilä, F. Massel, and M. A. Sillanpää, Phys. Rev. Lett. **118**, 103601 (2017).
[66] J. Y. Qiu, A. Grimsmo, K. Peng, B. Kannan, B. Lienhard, Y. Sung, P. Krantz, V. Bolkhovsky, G. Calusine, D. Kim *et al.*, Nat. Phys. **19**, 706 (2023).
[67] R. W. Heeres, P. Reinhold, N. Ofek, L. Frunzio, L. Jiang, M. H. Devoret, and R. J. Schoelkopf, Nat. Commun. **8**, 94 (2017).
[68] P. Scarlino, J. H. Ungerer, D. J. van Woerkom, M. Mancini, P. Stano, C. Müller, A. J. Landig, J. V. Koski, C. Reichl, W. Wegscheider, T. Ihn, K. Ensslin, and A. Wallraff, Phys. Rev. X **12**, 031004 (2022).